D6.3 Time Resolved Spectroscopy

Gavin D. Reid

Department of Chemistry, University of Leeds, Leeds LS2 9JT, UK. Email: g.d.reid@chemistry.leeds.ac.uk URL: http://www.chem.leeds.ac.uk/people/reid.html

Klaas Wynne

Department of Physics, Strathclyde University, Glasgow G4 0NG, UK. Email: klaas.wynne@phys.strath.ac.uk. URL: http://dutch.phys.strath.ac.uk/FRC/

CONTENTS

D6.3.1 Introduction

Following a short introduction on laser technology, in this chapter we shall describe how pulses of light at almost any frequency from x-rays to terahertz (THz) can be applied to problems in chemistry, biochemistry and physics. As predicted a decade ago,[1] the production of femtosecond pulses has led to many new and fascinating observations. Indeed, the number of applications of ultrafast lasers is already large and will only grow; an electronic search of Chemical Abstracts® for the terms 'femtosecond' and 'ultrafast' yields 19 000 references and obviously it would be impossible to describe all of these in the limited space available here, even if it were possible to become familiar with them all! The first attosecond pulses are now being made [2-7] and there is even a proposition for the generation of zeptosecond pulses.[8] As such, the future of time resolved spectroscopy appears to be brighter than ever.

Ultrafast lasers, of course, allow time-resolved experiments with which one can observe transient species. However, another important property is that with modest energy, they can have huge peak powers. This also makes femtosecond pulses suitable for many tasks we would not normally think of as being 'time resolved', including laser ablation of materials,[9] multi-photon absorption (for imaging of biological materials),[10] fragmentation (for example, of DNA into fragments that may be analysed using mass spectrometry),[11] the conversion to a range of new wavelengths using nonlinear techniques, (see chapter C3 Frequency Conversion and Filtering) as well as in producing pulses of electrons or even neutrons (see below) etc.

Femtosecond pulses have proven advantageous in a number of applications. When these lasers are used for machining for example, the resulting cuts are much cleaner because the laser pulses turn the material immediately into plasma, whereas longer pulsed lasers had caused materials to boil and sputter and hence damage the surrounding area. In this application, femtosecond lasers seem particularly adaptable to micro-machining techniques[12] and are being used in areas from corrective eye surgery[13,14] and dentistry[15-17] to the etching of glass and polymer substrates in the fabrication of 'lab on a chip' devices.

Since self mode-locking in titanium-sapphire was discovered in 1990 by Wilson Sibbett and his group in St Andrews,[18] there has been a revolution in time resolved spectroscopy, primarily as a result of the rapid commercialisation of ultrashort pulse technology (see **C2.3 Ultrashort Pulses**.) Also, in parallel with improvements in oscillator design, the technique of chirped pulse amplification, CPA [19] using solid-state gain media in regenerative or multipass schemes, has greatly simplified amplifier construction.

Ti:Sapphire is the gain medium for the vast majority of short-pulse oscillators and amplifiers, yielding pulses at around 800 nm, the fundamental wavelength, with pulse widths as short as 4 −5 fs. Sub 20 fs pulses have also been obtained from Cr^{4+}:YAG,[20] Cr^{3+}:LiSAF,[21] and Cr^{4+}:forsterite-Mg_2SiO_4 [22] in the near infra-red, which is a more useful wavelength range for applications such as high spend communications using optical fibres and photonic devices. New applications have also been found for these lasers in biomedical imaging[23] and optical tomography[24] for example.

In many cases, the output of short pulse lasers must be amplified for use in time resolved experiments (**D10.1** High Power Lasers for Plasma Physics). The extremely high peak powers involved complicate the amplification of nanojoule level, femtosecond pulses to the millijoule level and above. The choice of amplifier depends to a large extent on the application, the energy required, the repetition rate and the pulse duration and a wide range are available commercially. Typical operating parameters of Ti:sapphire amplifiers are 4 μJ at up to 250 kHz, 1 mJ at 1 kHz and 100 mJ or greater at 10 Hz. The amplifiers can be separated into two families, regenerative types in which a pulse is made to resonate in a stable optical cavity and multi-pass types where a pulse travels repeatedly through the pumped region of a gain medium along different paths.[19,25-32]. If the standard pulse width > *ca* 50 fs, available from commercial amplifiers is insufficient then home built amplifiers or specialist products are capable of improved performance, 20 fs or better. Amplifier technology is now relatively mature and has been discussed at length in recent reviews [33-35] but for state of the art designs see [36-38]

D6.3.2 Pump-probe Techniques

Even fast electronic devices cannot measure transients much faster than about a nanosecond and while there are specialised photodetectors such as streak cameras or avalanche photodiodes that can resolve picosecond or even 100's of femtoseconds transients in real-time, generally alternative detection techniques are required. The techniques that are used most frequently are based on the auto- or cross-correlation of two beams of femtosecond pulses. If the "sample" is a nonlinear crystal used for sum-frequency generation, this technique can be used to determine the shape and relative arrival time of two short pulses. If the sample

contains molecules or atoms that resonantly absorb the incident radiation, the experiment is a pump-probe experiment, an updated version of the flash photolysis experiment of Porter.[39]

The vast majority of ultrafast spectroscopy experiments use the pump-probe technique. The pump beam is typically much stronger than the probe, the two beams have a different centre wavelength and the femtosecond time resolution is obtained by sending one of the beams through a motor-driven optical delay line. The (relatively) strong pump beam initiates some process of interest, for example, a chemical reaction. The probe beam, entering the sample at later time delay, will be amplified, attenuated, or refracted because of the changes taking place in the sample. There are so many variations of this scheme and literally thousands of experimental examples, that it would be pointless to list them all. Therefore, two examples of the pump-probe technique will be described in some detail here to convey the general idea.
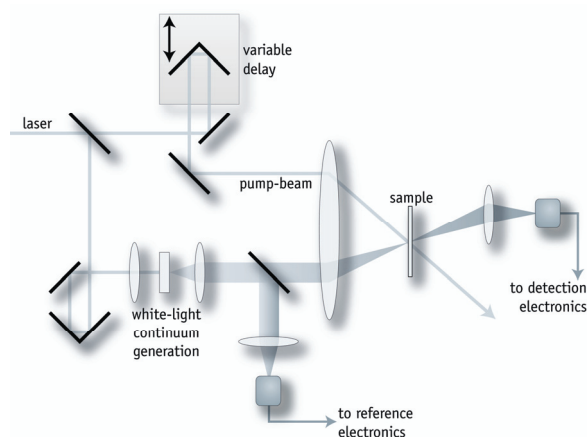

Figure 1. *A pump beam is sent through an optical delay line and focused into the sample. A fraction of the pump beam is split off and converted to another wavelength. In this example, a white-light continuum is generated as a probe, which is sent through another optical delay line and into the sample. After the sample, the white-light probe is spectrally resolved before being detected by a "slow" detector.*

Figure 1 shows a typical pump-probe arrangement. A relatively strong pump beam is sent through a variable (motorised) optical delay line and focused into the sample, where it initiates a chemical reaction or physical change. A small fraction of the pump beam is split off by an optical beam splitter and converted to another wavelength. In this example, a white-light continuum[40] is generated as a probe but one could also use other conversion techniques such as harmonic generation or parametric amplification to make probes at widely varying wavelengths. The probe pulse is sent through another optical delay line and focused into the sample. One may temporarily replace the sample by a nonlinear crystal to determine at which setting of the optical delay lines the pulses overlap in the sample by recording the cross-correlation response. In Figure 1, the white-light probe is spectrally resolved by a spectrometer after the sample in order to measure the transient transmission spectrum of the sample. The signal measured as a function of the pump-probe delay time reflects the creation and destruction of transient species in the sample. However, on short time scales (about < 1 ps), there are numerous phenomena such as cross-phase modulation that may complicate the signal. [41,42]

In the above example, both the pump and probe were laser pulses. However, lasers can also be used to make pump and probe pulses of an entirely different kind. Figure 2 shows an example where femtosecond laser pulses are used to generate, and gate, voltage pulses. [43-47] A short laser pulse can be used to create carriers in the conduction band of a semiconductor and thereby create a femtosecond voltage pulse that can be sent down a transmission line deposited onto the sample. This voltage pulse can then be picked up using an STM tip. Gating the current flowing through the STM tip using a second laser pulse, the averaged tunnel current can be measured as a function of pump-probe delay in addition to the spatial position of the tip. Therefore, this type of pump-probe technique provides both very high temporal resolution as well as spatial resolution. There are many other examples of "unconventional" pump-probe techniques. The probe may consist of x-ray pulses, electron pulses or any other kind of pulsed particle beam (see section D6.3.12). The only critical requirement is that the pulses in the pump beam are synchronized, with minimum jitter, to those in the probe beam.
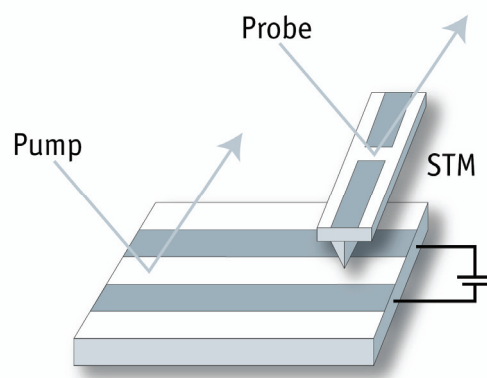
Figure 2.   *"Unconventional" pump-probe technique. In this example, the pump beam excites electrons in the conduction band of a semiconductor thereby creating a femtosecond voltage pulse in the metal transmission line deposited on top of the semiconductor sample. The voltage pulse can be measured by an STM tip. If the current flowing through the STM cantilever is itself gated by a probe pulse, time and space-resolved measurements can be performed.*

D6.3.3 Terahertz-Pulse Generation and Detection

Femtosecond IR pulses can be generated using parametric down-conversion in an Optical Parametric Oscillator (OPO) or Amplifier (OPA). As the crystals used in typical OPAs such as BBO, $LiNbO_3$, $AgGaS_2$, are opaque in the far-IR region, standard down-conversion methods cannot produce pulses with a wavelength longer than ~18 μm. However, long-wavelength pulses can be generated (and detected) using so-called terahertz techniques.[48] There are two methods for generating sub-picosecond THz (10^{12} Hz) pulses: *Photoconduction* and *optical rectification*. In photoconduction, a laser pulse incident on an absorbing semiconductor creates (real) charge carriers in the conduction band. Acceleration of these carriers in an electrical bias field gives rise to a transient photocurrent that radiates electromagnetic waves. In the far field, the radiated electric field is approximately given by[49] $d\vec{j}_S(t)/dt$, where $\vec{j}_S(t)$ is the time-dependent surface current. This method is typically used in conjunction with an antenna structure (see Figure 3a), which allows an external DC bias field to be applied. An antenna structure ideally suited to be used with low-power mode-locked lasers was developed in the 1980s at Bell Labs[50] and IBM,[51] and is now the most common method for generating and detecting THz pulses. In such a set-up, two metal electrodes are laid down on a silicon or GaAs substrate, typically with a separation of ~100 μm. A beam of femtosecond laser pulses is focused between the electrodes, in a spot with a diameter of a few micrometres. On the generation side, the metal electrodes are biased with a few tens of volts and the excitation by the pump laser triggers the emission of THz radiation. On the detection side, the incident THz beam accelerates carriers created by another visible beam, resulting in a measurable photocurrent. Since the visible beam has to be focused to a very tight spot in this method, only unamplified ultrafast lasers can be used. There is no overriding reason, however, why one should use such closely spaced electrodes. Large-aperture photo-conducting antennas work very well for the generation of THz pulses when pumped by amplified pulses. The conversion efficiency can be as much as ~0.1%. With low repetition rate (10-1000 Hz) ultrafast laser systems, far-infrared pulses with energies as high as 1 μJ have been generated.[52] It was recently reported that high-power pulses can even be used to generate THz pulses by generation of ions and electrons in electrically-biased air[53] or by four-wave mixing in air.[54] Superluminal fronts have been produced in miniature photo-conducting capacitor arrays in order to produce THz pulses.[55,56] It is even possible to generate THz pulses by laser-induced electron-transfer in dissolved dye molecules with an external DC bias applied,[57] however, this appears to be more a curiosity than an efficient generating technique. Pulse-shaping techniques have been used to make high-power THz pulse trains[58] and narrow band THz radiation. [59]
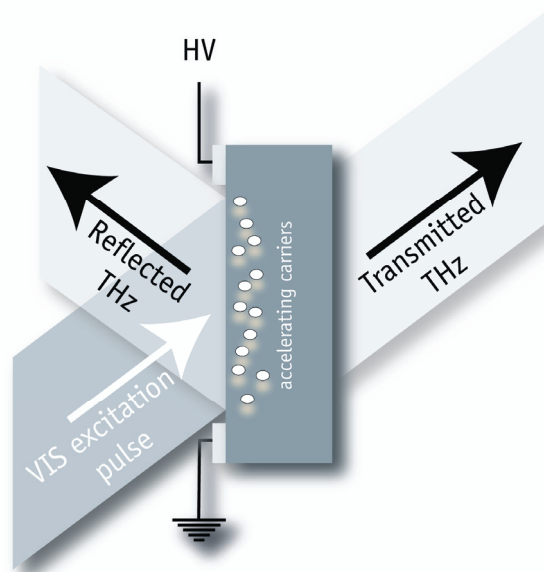
Figure 3. *(Left) Schematic diagram illustrating the generation of terahertz pulses. A visible femtosecond input pulse irradiates a semiconductor antenna and creates conduction electrons. The acceleration of these electrons in an external DC field results in the emission of two beams of terahertz pulses. (Right) THz pulses generated in various ways and detected in a 0.5-mm long <110>-cut ZnTe crystal by a 40-fs pulse at 800 nm/1 kHz. "Antenna" is a pulse generated in a large-area DC biased antenna. "ZnTe" is a pulse generated in a 0.5-mm ZnTe crystal. "MBA-NP" is a pulse generated in a 0.3-mm c-cut 2-(a-methylbenzylamino)-5-nitropyridine crystal.*

An external bias field is not strictly necessary for photoconductive generation of THz pulses, as real carriers generated by a visible laser pulse can be accelerated in the field of the depletion layer of the semiconductor. This surface field will accelerate the carriers perpendicular to the surface of the semiconductor and hence the THz oscillating dipole will be perpendicularly to the surface. Therefore, THz radiation generated through this effect is only observed if the angle of incidence of the exciting visible laser beam is nonzero. Typically, the effect maximises at Brewster's angle.

Optical rectification is distinct from photoconduction, in that the visible exciting beam creates virtual rather than real carriers. A more appropriate way to describe this is that the second-order susceptibility, $\chi^{(2)}$, of the crystal is used for difference-frequency mixing. Thus, the second-order polarisation can be written in the time domain as $P_{THz}^{(2)}(t) = \varepsilon_0 \chi^{(2)} E_{VIS}(t) E_{VIS}^*(t)$, which shows that in the near field, the electric field of the THz pulse has the same shape as the intensity envelope of the visible exciting pulse. Optical rectification takes place in any non centro-symmetric crystal including some highly nonlinear organic crystals and poled polymers. [60-63] In the last few years, it has been discovered that optical rectification is an efficient method for generating THz pulses if used appropriately. Since a sub-picosecond THz pulse has a spatial length comparable to its centre wavelength, it travels through a material at its phase-velocity. Therefore, for optimum conversion from visible to far-infrared wavelengths, one has to match the *group velocity of the visible pulse* with the *phase velocity of the THz pulse*.[64-66] This condition is met in some zincblende, large band-gap semiconductors such as ZnTe and GaP when the exciting laser has a centre wavelength of *circa* 800 nm. Still, the conversion efficiency tends to be on the order of 10^{-5},[6] which is inferior to photo-conductive generation techniques.

The "inverse" of optical rectification is electro-optic sampling: A THz pulse incident on an electro-optic crystal such as ZnTe will induce a birefringence through the Pockels effect. An ultrafast visible probe pulse with a variable delay co-propagating through the same crystal will experience a retardation that can be retrieved with balanced detection. Scanning the relative time-delay of the probe pulse, one can record a time-domain trace of the electric field of the THz pulse. Using this method, signal-to-noise ratios, defined as the ratio of the THz pulse-peak to the noise background, as high as 10^7 have been reported.[67] However, the signal-to-noise ratio with which one can measure the peak of the THz pulse is typically on the order of 10^2-10^3 in 100 ms. Techniques for measuring a THz pulse in a single shot have recently been developed. [68,69] Comparisons show[70] that when high repetition-rate (~100 MHz) lasers are used, electro-optic and photo-conductive sampling are

about equally suitable for detecting THz pulses. However, electro-optic sampling appears to be the only useable technique for lower repetition-rate (~1 kHz) lasers.

As rectification and electro-optic sampling are non-resonant effects, the minimum duration of the THz pulses that can be generated or detected is only limited by the thickness of the crystal scaled with the difference in phase and group-velocity. Thus, with *circa* 10-15 fs exciting pulses at 800 nm, it has been shown that THz pulses could be generated with detectable frequencies as high as 70 THz.[71] In contrast, with photoconductive sampling the maximum detectable frequency is about 20 THz[72] and typically much lower. This method also works with high-power low repetition-rate lasers.[6] At these large bandwidths, it is unavoidable that the THz-pulse spectrum will overlap with a phonon absorption band in the generating and detecting crystals, leading to large oscillations in the THz field trailing the main peak.

The current record highest detectable frequency for a THz pulse is ~70 THz but there is no reason to believe that this could not be improved upon. Using the time-bandwidth relation $\Delta \nu \cdot \Delta \tau = 0.32$, it follows that with the shortest visible pulses achievable, *circa* 4-5 fs, usable power at frequencies from 0 to 160 THz ($\lambda = 1.8\ \mu m$) could be achieved. As femtosecond lasers continue to shrink in size, ultrafast THz devices may well take over from Fourier transform infrared (FTIR) spectrometers as general-purpose IR spectrometers. As an entire THz time-domain trace can be acquired in a single shot, [68,69] these devices would combine the reliability and accuracy of FTIR with real-time speeds.

It is true that THz pulses give relatively easy access to a region of the electromagnetic spectrum that used to be hard to study. Unfortunately, absorption bands in the THz region tend to be extremely broad (at least in the condensed phase) and therefore it tends to be difficult to extract meaningful information from THz absorption spectra. THz absorption spectroscopy has been used in the past few years to study liquid dynamics[73,74] and the dynamics of charge carriers in semiconductors. [75-77] One of the most interesting aspects of THz pulses is that it is possible to measure the electric field of the pulse directly and how it changes on propagation through some optical system. This property has been applied, for example, to study the propagation of evanescent waves and superluminal propagation of light. [78-82] It has also been used to great effect for THz imaging and object reconstruction.[83-85] Because THz pulses from large-area antennas are half-cycle in the near field, they can be used as powerful quasi-DC electrical pulses that can, for example, ionise Rydberg atoms.[86,87] Because THz pulses are automatically synchronised to a visible ultrafast laser (unlike the far-infrared pulses from a free-electron laser), they can be used for pump-probe spectroscopy. For example, visible-pump THz-probe spectroscopy has been used to study carrier dynamics in semiconductors,[88-91] superconductors and liquids.[92-96]

D6.3.4 Emission Techniques

Time resolved emission measurements are performed using one of two techniques, time correlated single photon counting (TCSPC) or fluorescence up-conversion using a non-linear crystal. The TCSPC method is much the more common and the literature contains myriad examples, but the technique is limited to a time resolution >20-50 ps and the data obtained are often seriously compromised by convolution with the instrument response function. Consequently, the up-conversion technique, which lacks the sensitivity of TCSPC, is favoured when studying shorter-lived processes.

D6.3.5 Time Correlated Single Photon Counting

TCSPC is well described elsewhere.[97-100] The sample is repetitively excited at ca 1 MHz by a pulse train from a mode-locked oscillator. The laser light is detected by a fast photodiode, which is used to signal the beginning of the experiment. This pulse initiates a voltage ramp on a time-to-amplitude converter (TAC) and the ramp is stopped on the arrival of the first photon after the excitation event from the sample. A constant fraction discriminator (CFD) is typically used to differentiate between background noise and the single photon signal from the detector (usually a fast proximity type, micro-channel plate photomultiplier tube MCP-PMT). The voltage, so obtained from the TAC, is a linear function of the elapsed time between the start and stop events. This voltage level is then converted to a time channel by a multi-channel analyser (MCA). The event is binned to form a histogram of counts versus channel number (time) over many millions of excitation events. The histogram represents the decay of the excited state convoluted with the instrument response function. Figure 4 shows some representative data from the fluorescence of N-acetyl L-tryptophanamide in water.
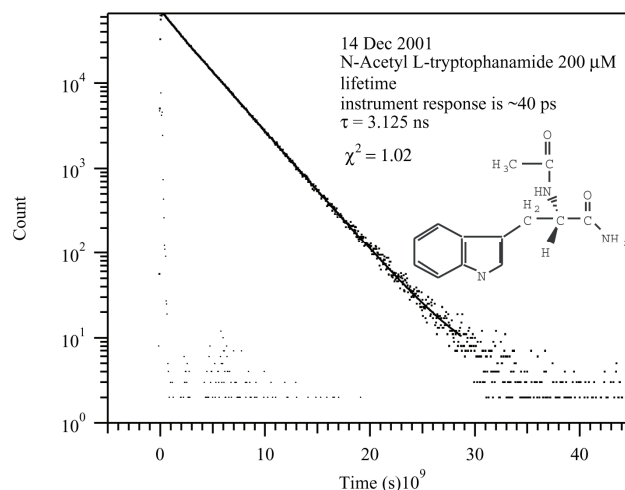
Figure 4. *Time-correlated single photon counting measurement of the lifetime of N-acetyl L-tryptophanamide in water showing the data (dots) and the instrument response function (circles). Data courtesy of Veysel Kaiser (University of Leeds)*

Traditionally, the excitation source would have been a picosecond, cavity dumped dye laser synchronously pumped by a modelocked argon ion or Nd:YAG laser. Dye laser technology has now largely been superseded by the use of solid-state lasers, Ti:sapphire in particular. The CFDs, TAC and MCP can also now be purchased on a single computer board, greatly simplifying the instrumentation.

D6.3.6 Fluorescence Lifetime Imaging Microscopy, FLIM

Fluorescence lifetime imaging produces a 2-D map of a sample based on the distribution of measured fluorescence lifetimes at each position in the sample, using a microscope equipped with high frequency modulation[101,102] in the frequency domain or, better, a nanosecond gated, multichannel plate image intensifier [103,104] and the lifetimes are calculated on a pixel by pixel basis. It might be imagined that a simple measurement of intensity versus position would provide sufficient information. However, intensity analysis requires knowledge of the concentrations of each species present. Real world samples may also be turbid or signal size may depend on optical alignment. If the assumption is made that the sample is composed of discrete emitters whose fluorescence lifetime is exponential, an analysis that is independent of intensity can be made. For a review see Szmacinski and Lakowicz[105] There has also been recent progress on the analysis of more complex decays.[106,107]

FLIM is often used in conjunction with fluorescence resonance energy transfer, FRET.[108] FRET is the transfer of energy from the initially excited state (the donor) to an acceptor due to Förster dipole-dipole energy transfer. The rate of transfer depends on the spectral overlap between the emission spectrum of the donor and the absorption spectrum of the acceptor, the fluorescence quantum yield of the donor, the relative orientations of the transition dipole moments and the distance, d, between the donor and acceptor, which has a $1/d^6$ dependence. This allows a probe of the local environment of the donor, since FRET will change the observed fluorescence lifetime in a manner that depends intimately on the local environment. It is the last property, the distance dependence that has led to the most common application of FRET, the measurement of the distance between donor and acceptor in tagged molecules. For example, the dynamics of protein folding and unfolding have been observed by following the FRET in fluorescently tagged peptides.[109,110] In an elegant study by Ng *et al.,*[111] a dynamic marker of protein kinase Cα (PKCα) activation was exploited. Activation of PKCα was detected through the binding of fluorescently tagged phosphorylation site-specific antibodies and the corresponding FRET was measured through the donor fluorophore on PKCα by FLIM. This experiment demonstrated that FLIM could be used to detect the catalytic function in-vivo.

D6.3.7 Time-Resolved Single Molecule Microscopy

While TCSPC or FLIM usually measure the average fluorescence lifetime from an ensemble of molecules, the last decade has seen the integration of TCSPC with microscopy in such a way that single molecules within the condensed phase, whether it be solution, polymer, crystal or protein, can now be observed routinely as a

function of time.[112] Thus, molecular recognition by an environment sensitive fluorescent probe can allow for the observation of specific individual molecular states rather than an ensemble average. For recent reviews see references [113,114]. From such measurements, we now know that the properties of single molecules such as fluorescence intensity, spectral shape and position, fluorescence lifetime, intersystem crossing rate and triplet lifetime fluctuate in time, showing us that the conformation of the molecule or the chemical or physical environment in which it resides, influence the photophysics. One problem in utilising FRET detection is knowing the orientation of the dipole moment and recent work has shown that there can be discrete jumps in absorption dipole orientation.[115]

The primary experimental difficulty in single molecule detection is the separation of the desired fluorescent photons from the background Rayleigh and Raman scattering and impurity emission. The background signal will be proportional to the excitation volume and therefore this needs to be minimised. A confocal, epi-illuminated microscope is often employed, where the excitation spot is a diffraction-limited area determined by the focus of a high numerical-aperture objective lens, see Figure 5. The same objective lens is used to collect the emitted light, which is focussed through a small aperture (typically 20 µm) and onto a detector, usually an avalanche photodiode (APD) of high quantum efficiency and rapid temporal response. APD packages including discriminators can be purchased providing a TTL pulse for each single photon event. The aperture acts as a spatial filter and so passes only those photons that originate from the focal point *i.e.* it reduces the depth of field thus removing weak fluorescence derived from those molecules below and above the focus, as well as scattered light. If the APD is sufficiently small, it may itself act as the aperture easing alignment sensitivity. Since fluorescent photons are red shifted from the excitation wavelength, due to (vibrational) relaxation in the excited state, a simple filter can be used to separate the emitted photons from any remaining scattered light. The spatial resolution is limited to about 100 nm but can be further enhanced by using two-photon excitation. If the sample is sufficiently dilute (10^{-10} mol dm^{-3}) then statistically, only a single molecule will occupy the excitation volume at any one moment. On the other hand, if the molecules are free to diffuse then molecules will move in and out of 'view' resulting in bursts of fluorescence signal which are discriminated from the background using the technique of burst-integrated fluorescence lifetime, BIFL.[67,116-118] Other photophysical processes also result in intensity fluctuations including time dependent shifts in the fluorescence spectrum,[75,119] triplet formation,[120] which results in 'blinking', a period of darkness while the triplet state relaxes, and irreversible bleaching.[112] Therefore the analysis of the time resolved fluorescence requires great care.
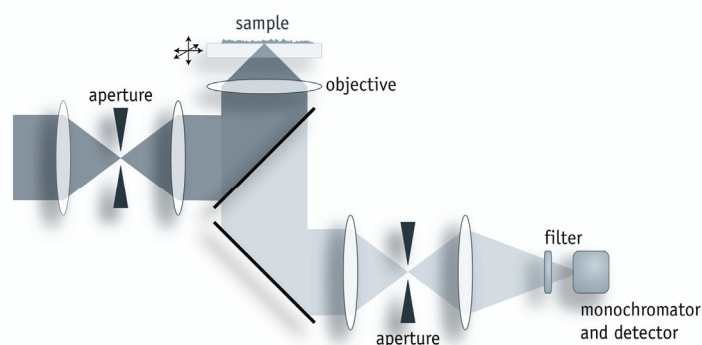

Figure 5.   *Schematic of a confocal microscopy apparatus. The laser profile is cleaned up through a spatial filter and reflected from a dichroic beamsplitter through a high numerical aperture objective onto the sample. Fluorescence is collected back through the objective, imaged onto a second aperture and focused onto a avalanche photodiode detector.*

By way of illustration, recent work from Talaga et al [121] has shown the trajectories of a small peptide undergoing folded to unfolded transitions by single molecule FRET. The observation of a single protein domain in dynamic equilibrium between folded and unfolded states is extremely exciting. The terminal ends of a peptide, a two stranded coiled-coil subunit from the yeast transcriptase factor GCN4, were labelled with rhodamine 6G (donor) and texas red (acceptor) and the FRET signal was used to determine the end-to-end separation of the tags, this being a direct probe of the path between the folded and unfolded states.

D6.3.8   Fluorescence Upconversion

Upconversion is a derivative of the pump probe technique, see Figure 6. The laser (often the second harmonic of a Ti:sapphire oscillator) is split such that part of the beam excites the sample and the fluorescent photons are detected by sum frequency generation with a short gate pulse in a non-linear crystal.[122] For the best temporal resolution, the fluorescence is often collected using a reflecting microscope objective, or off-axis parabolic or elliptic reflectors, in place of refractive optics. The resultant signal is separated from any scattered gate photons using a collection of filters and a grating monochromator (sometimes double grating) and detected using a photomultiplier tube. By scanning a delay line between the gate and the excitation event, the fluorescence decay can be built up point by point as in a pump probe experiment and by scanning the phase matching angle of the upconversion crystal, the full emission spectrum can be obtained. Unfortunately, small changes in optical alignment result from a change in crystal angle and for this reason, the upconversion technique is considered to be experimentally difficult and the full spectral method is somewhat tedious. The technique has however, been used extensively and is the only emission technique with true femtosecond resolution. Ideally, the upconversion method requires a high repetition rate, low energy source but examples of data collected at a 1 kHz rate are known. We give references to illustrative examples from the recent literature.[123-126]. A new method for upconverting the entire fluorescence spectrum without realignment of the optical elements has recently been proposed and while not yet perfected, seems very appealing.[127].
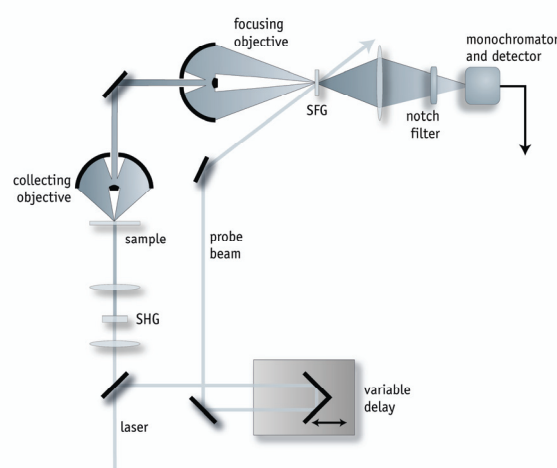

Figure 6.   *A schematic of a fluorescence upconversion experiment. Fluorescence from the sample excited by the second harmonic of a Ti:Sapphire oscillator is collected and focused onto a frequency doubling crystal, where a portion of the laser light is used to time-gate the fluorescence by sum frequency generation (SFG).*

In a pump-probe experiment, the loss of the excited state is often observed by following the decay of the stimulated emission signal. Often, however, this is not possible or the resulting signal remains ambiguous as to its origin due to competing signals from transient or ground state absorption. In these cases it is desirable to measure the emission directly. Figure 7 shows the oscillatory fluorescence from a charge-transfer complex hexamethylbenzene with TCNE[128] and the vibrational wavepacket is similar to that observed in the excited state of the TCNE:pyrene complex (see Figure 10 below). Deconvolution of a TCSPC decay with a known instrument response function is incapable of such resolution.
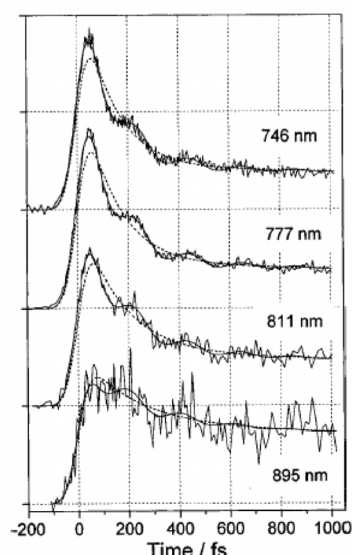
Figure 7. *Oscillatory emission from the charge transfer complex of hexamethyl benzene and tetracyanoethylene. Reprinted with permission from reference* [128] © *1997 American Chemical Society.*

D6.3.9 The study of fast chemical reactions

Ultrafast spectroscopy has become one of the most active areas of physical chemistry. Rather than postulating mechanisms for chemical and biological reactions, ultrashort laser pulses can now be used to observe and even control the outcome of reactions in real time.

In the 1980s and 90s, a series of experiments were performed by a number of groups, which came to be known as "femtochemistry" or "femtobiology." Impulsive excitation of a molecule results in a wavepacket that is initially *localised* in the Franck-Condon region of the upper surface. The wavepacket is the superposition of characteristic frequencies corresponding to the energy differences between coherently excited vibronic states where importantly, the spatial resolution of the wavepacket is not lost due to the uncertainty principle.[129] The wavepacket, behaves as a classical particle in that it has a well-defined position and group velocity (speed) and will evolve on the excited state potential moving along the Franck-Condon direction,[130-132] see Figure 8. Since the wavepacket 'explores' much more of the potential surface than simply the Franck-Condon region, its time dependent behaviour provides a wealth of information about the surface(s).
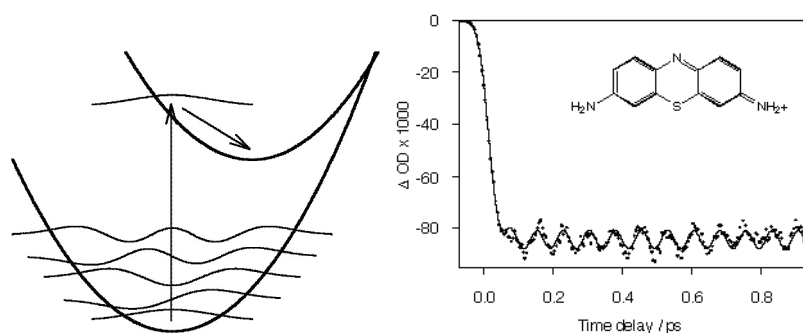

Figure 8. *(Left) Schematic diagram of a vibronic transition excited by a pulse whose width is smaller than the vibrational period. The pulse creates a coherent vibrational wavepacket in the excited electronic state that will oscillate in the excited-state potential well. (Right) Time-resolved 600-nm-pump 700-nm-probe signals in the dye molecule thionine studied with 40-fs time-resolution. The signal is stimulated emission from the excited electronic state and the oscillations correspond to a vibrational mode at 443 cm^{-1} in the excited-state potential.*

In the gas phase, the wavepacket will eventually lose phase coherence and dissipate, due to both the anharmonic nature of the potential surfaces and coupling between vibrational modes. As it happens, the

timescale for dephasing is longer than that of nuclear motion and the wavepacket remains intact for many periods of vibration and so will survive for sufficient time to enable detailed study.[133] Even though the wavepacket eventually disperses, it has the remarkable ability to rephase [134] at some later time and this property has been exploited in isotope separation for example[135] since the recurrence time will depend on the mass of individual isotopes.

In the condensed phase, dissipative interactions of either inter- or intra-molecular nature can lead to a rapid loss of phase coherence among the nuclear eigenstates that make up the wavepacket. Sometimes the wavepacket motion is strongly damped but on other occasions, it remains intact for many picoseconds. Chemists are particularly interested in the chemical products formed as a result of crossing from one potential energy surface to another. In the strongly damped case, the decay of the population is monotonic and tells us little about the nature of the reactive nuclear dynamics. However, if the dissipative reactions are weak, then the nuclear motion is underdamped and the wavepacket may repeatedly sample the surface-crossing region. Each visit to the crossing region results in some product being formed and it will therefore appear in a step-wise manner with a frequency corresponding to the period of the wavepacket motion. In most molecules of chemical interest, several vibrations couple both to the optical transition and to the curve crossing. In such cases, excitation of two or more modes leads to an evolving, multidimensional wavepacket and the short time dynamics will depend on the extent to which the Franck-Condon modes project onto the modes that couple to reaction coordinate *i.e.*, the promoting modes.

The "hydrogen atom" of femtochemistry is the diatomic molecule NaI. Non-adiabatic transitions in this molecule have been studied extensively in the gas phase. [130] When NaI is excited by a femtosecond UV pulse (Figure 9), a wavepacket is created on the repulsive side of the potential in the excited state, which (at large interatomic distances) corresponds to the ion pair Na^+ and I^-. However, this repulsive potential forms an avoided crossing with the ground-state potential, which (at large interatomic distances) corresponds to the radical pair Na + I. If the molecule is probed in the excited-state potential well, the wavepacket is observed to oscillate, with the signal intensity diminishing with each period. However, if the sodium radical is probed by inducing fluorescence with the probe pulse, the population of the radical is observed to increase in a stepwise fashion. Such an experiment shows that the chemical reaction (a dissociation in this case) is a quantum-mechanical process in which a fraction of the bound wavepacket tunnels to the state of dissociated radicals each time the wavepacket travels through the crossing region.

Interestingly, it is possible to use quantum mechanical interference of wavepackets to steer a reaction in a desired direction and away from undesired pathways,[136-142] often referred to as coherent control. The idea of using lasers to control chemical reactions is an old one.[143,144] Progress in the field though was limited for many years because of both the computational difficulty of solving Schrödinger's equation with sufficient accuracy to know how to shape the pulses to produce the desired effect, over and above the technological problem of producing light modulated on the femtosecond timescale. However, a general approach where the required pulse shapes are derived empirically from experimental feedback[145,146] has been shown capable of learning how to cleave selective bonds in organic molecules such as acetone [147] and organometallic compounds[148] as well as optimising laser induced fluorescence[145] and stimulated Raman emission.[149]
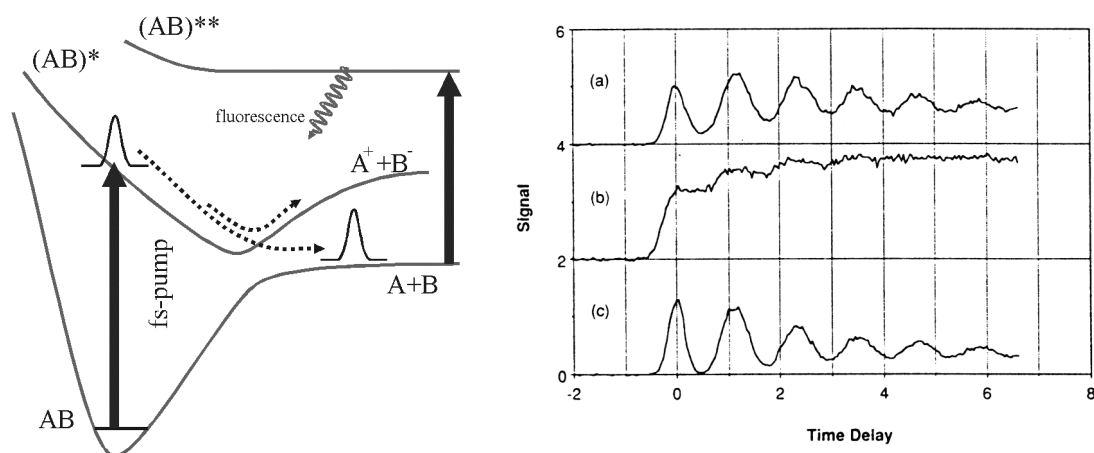

Figure 9. (Left) Simple diagram depicting a typical coherent dissociation reaction. The pump pulse excites a small molecule to its first excited state. If the pump pulse is shorter than the vibrational period, it

may create a coherent wavepacket that will oscillate in the excited state potential well. In this diagram, the molecule splits into two fragments either consisting of two radicals or two ions. A probe pulse excites the molecule to a third state, from which it fluoresces back to the ground state. The total fluorescence is measured as a function of pump-probe delay. (Right) Pump-probe results from NaI with λ_{pump} = 310 nm. (a) λ_{probe} = 580 nm; (b) λ_{probe} = 589 nm (on resonance); and (c) λ_{probe} = 612 nm. Reprinted with permission from reference [100] © 1988, Elsevier Science B.V.

A study, such as the one on NaI described above, becomes even more interesting if one can compare the behaviour in the gas phase with that in solution.[150] A number of molecules that had been studied in the gas phase have now been studied in solution where again one could observe quantum beats due to vibrational wavepackets. Examples are HgI, [151,152], I_2^- and I_3^- [153-156] and I_2 [157,158] in solution or in small clusters [159,160]. Vibrational quantum beats have now been observed in a large variety of molecules in the condensed phase including proteins.[161] In these large complicated systems, quantum beats provide a unique opportunity to determine the potentials relevant for chemical and biological reactions. Not least, the femtochemistry technique may be used to detect short-lived intermediates that would be invisible when ordinary spectrally resolved techniques are used.

In an experiment analogous to the coherent appearance of products in the NaI photo-dissociation reaction, coherence in a solution-phase reaction has also been observed.[162] In one example, vibrational wave packet motion was created in the excited charge-transfer state of the 'Mulliken type' electron donor–acceptor complex between tetracyanoethylene (TCNE) and pyrene by an ultrashort ~40 fs, 810 nm pump pulse. A new charge transfer (CT) absorption band appears when two molecules form a complex and the optical transition to the CT state causes a charge separation. The ground state recovers by a thermal electron transfer reaction back from this charge-separated state. The advantage in studying such reactions is that the Franck-Condon active modes in the absorption will be the same vibrational modes that couple to the back electron transfer reaction and in principle, these modes may be known from resonance-Raman spectroscopy. Observations of the dynamics of the TCNE–anion transient absorption and the disappearance of the bleach of the ground state absorption show that the electron-transfer reaction back to the ground state of the complex occurs on a 250 fs–1.5 ps time scale. The bleach recovery signal shows clear oscillations, Figure 10. Vibrational coherence was also monitored by observing quantum beats in the stimulated emission from the charge transfer state back to the ground state in the near infrared. This observation strongly suggests that the electron transfer reaction is indeed vibrationally coherent and that the reaction rate is modulated by this coherence i.e. the ground state is reformed in a step-wise manner.
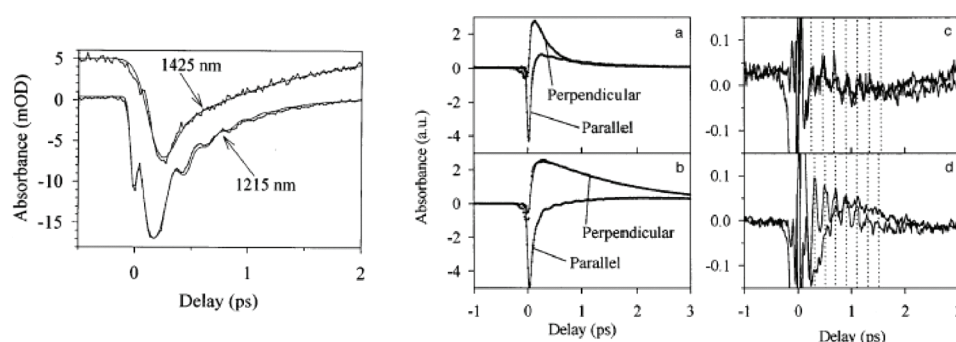

Figure 10.   *Vibrational coherence in the excited state of the TCNE:Pyrene complex as observed through the stimulated emission in the near infrared (left). This is responsible for the step-wise re-population of the ground state (right), shown enhanced by the residual plot (far right) Top is in acetonitrile solution and below in benzonitrile, where the reaction is a little slower.*

In a femtosecond pump probe experiment, vibrational dynamics, as we have seen, are recovered from wavepacket motion superimposed on the electronic signals. Another method is to follow a reaction or the response of a solvent or crystal lattice directly, either by time resolved resonance Raman scattering[163,164] or by using an infrared probe pulse. [41,165-167] Until effective non-linear crystals for infrared generation or upconversion became available in the past decade, time resolved infrared experiments were uncommon. In recent years,

however, infrared probes have been used successfully in monitoring organometallic chemical reactivity,[168-171] solvation and liquid dynamics,[172-174] biochemical applications,[175-177] electron transfer reactions[178] and in bulk and nanostructured semiconductors.[179] On longer timescales, Fourier transform techniques can be applied, principally step scan FTIR spectroscopy,[180,181] which can have a resolution of 10 ns in modern configurations.[182-187]

D6.3.10   Photon Echo Measurements

In principle, it might seem that there is no difference in the information that can be obtained from a frequency-resolved or a time-resolved experiment. In a frequency-resolved spectrum, a vibronic transition may show up as a series of sharp absorption lines. In the equivalent time-resolved experiment, one will observe quantum beats whose periods correspond to the inverse of the spacings between the absorption lines. In practice, however, there may be differences. For example, even in the gas phase, the spacing between the absorption lines may be so small that they are hard to resolve. In the solution phase, the molecule under study will couple to the degrees of freedom of the surrounding bath and most of these bath states will be coupled to the vibronic states in the molecule resulting in the broadening of the transition. In such a case, a spectrally resolved experiment will provide little information about the dynamics of the molecule or the dynamics of a chemical reaction that one would like to study. Similarly, a standard pump probe experiment is unlikely to tell us very much about the timescale of solvent fluctuations and their influence on a chemical reaction, yet fundamental theories, for example, of solvent assisted barrier crossing[188] and electron transfer reactions[189,190] require such information.

A variation on the pump-probe technique is the photon echo.[191-196] Figure 11 shows the so-called folded-box CARS geometry, which enables the simultaneous determination of a wide range of transient non-linear signals. The figure is in a plane (xy) after the sample perpendicular to the z direction of the almost colinear excitation beams (1,2,3). Experimentally, the intensity, I_i, of one of the twelve outgoing waves i, i = 1to12, of wavevector k_i is measured. Beams 4 to 6 are those resulting from diffractions of one of the three beams from a grating formed by the other pair (4-wave mixing); in particular, beam 4 represents the diffraction of the probe 1 from a grating formed by pump beams 2 and 3. The phase-matching conditions for these beams are $k_4 = k_1 - k_2 + k_3$, $k_5 = k_1 + k_2 - k_3$ and $k_6 = -k_1 + k_2 + k_3$. Beam 6 would represent diffraction of either 2 or 3 from a grating formed by the other pair but, as such, is present only when all three beams are time coincident and is a suitable instrument function to determine the ultimate temporal response of the system. Beams 7 to 12 are two beam self-diffraction or 3-wave mixing spots; in particular beams 7 and 8 result from the mixing processes: $k_7 = 2 k_1 - k_2$ and $k_8 = 2 k_2 - k_1$. In the excitation of inhomogeneously broadened systems, diffraction of beam 1 from a grating formed by beams 1 and 2 may be thought of as a photon echo and in modern language the four-wave mixing experiment described here is termed a three pulse echo. The folded box CARS setup also allows the detection of transient absorption, pump-probe signals with either beam 2 or 3 blocked whilst monitoring beam 1.

The echo signal of interest may be time integrated, time gated or heterodyne detected, all of which yield subtly different information about the response of the system. For applications and a full description of the different methods see for example reference [196].
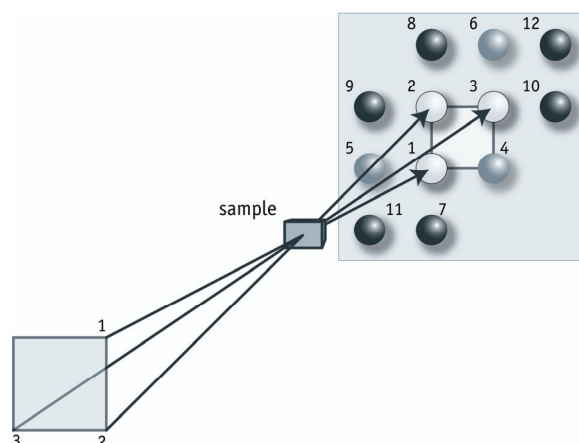
Figure 11.   *A folded-box CARS beam geometry for three-pulse photon echo experiments. A laser is divided into three parts labeled 1-3 which are focused into a sample from three corners of a square. The sample will radiate a fourth field in the direction of the momentum matched locations, 4-6.*

Vibrational frequencies are likely to be more sensitive to their local environment than electronic transitions and, therefore, recently photon echo techniques have been extended to use infra-red pulses.[177,197-199] Of particular note are the experiments from the Hochstrasser and Tokmakoff groups, who have both used two dimensional photon echo spectroscopy in a manner analogous to 2-D NMR. In particular, Hochstrasser has been able to determine the structure of a small peptide in solution from its 2-D IR spectrum.[200] These techniques appear to be extremely promising for future application.

D6.3.11   Femtosecond Mass Spectrometry

Femtochemistry has long been combined with mass spectrometry to provide mechanistic detail about chemical reactions.[131,201,202] Pump and probe laser beams are crossed with a molecular beam and ionised fragments are detected with a time-of-flight mass spectrometer as a function of pump-probe delay. Zewail's group at Caltech, has applied the technique to direct studies of the transition state of a chemical reaction.[203] The concept of concertedness has been tested in α-cleavage and retro-Diels-Alder reactions,[204-206] while recent work has focussed on elimination and Norrish 'type I' reactions.[206-209] The introduction of high repetition rate lasers allows new experiments in this area.

D6.3.12   Future Trends: X-Ray and Electron-Pulses for Ultrafast Structure Determination

Ultrafast time-resolved pump-probe spectroscopy has been used for two decades to study chemical, biological, and physical reactions. Spectroscopy relies on a careful and skilful analysis of transient UV-VIS or IR spectra to find out the nature of intermediates or reaction products. Probing with ultrafast infrared pulses can provide more direct information about the making and breaking of bonds[41] but no spectroscopic technique will ever provide direct and unambiguous information about the instantaneous positions of the atoms involved in a reaction. X-ray diffraction has been used for close to a century to determine the atomic structure of crystals. Especially in the life sciences this has resulted in a much better understanding of the structure of proteins and other biomolecules and hence to a better understanding of the fundamentals of biochemistry. Because of the great absorption of electrons by materials, time-resolved electron-diffraction experiments have so far only been performed in the gas phase and on surfaces. Clearly, it would be a great advantage if one could apply the technique of x-ray diffraction on a femtosecond timescale. Modern synchrotron facilities such as the European Synchrotron Radiation Facility (ESRF) in Grenoble and the Advanced Light Source (ALS) in Berkeley now make it possible to study structural dynamics using time-resolved x-ray crystallography on a (sub)nanosecond time scale. However, as many reactions take place on a picosecond or even femtosecond time scale, the race is on to produce femtosecond x-ray pulses with enough intensity for rapid acquisition of diffraction patterns. Over the last few years, huge progress has been made in the technology of producing femtosecond x-ray pulses. These new sources have allowed the first few simple time-resolved diffraction experiments to be performed.

Nonlinear crystals typically used for second or third harmonic generation, are useless for generating radiation in the deep UV, let alone the x-ray region. However, high harmonic generation in low-pressure gases has been used successfully to generate femtosecond deep-UV and soft x-ray pulses. A new direction of research is the application of capillary or corrugated waveguides to achieve phase-matching for high-harmonic generation. For example, a glass capillary has been used[210] to modify the phase-matching condition for coherent soft x-ray generation. Using this set-up, femtosecond pulses at 800 nm were converted to the 17 to 32 nm wavelength range (~30th harmonic) with about 0.2 nJ energy per harmonic order. Extremely short (5 fs) amplified laser pulses have been used[211] to generate x rays (~4 nm) in the water window by harmonic generation in a gas jet. The advantage of very high harmonic generation is that the x rays are generated in a well-collimated beam. The disadvantage is that it has not been shown to be possible yet to generate hard x rays with wavelengths smaller than a molecular bond length required for diffraction experiments.

Developments in chirped-pulse amplification have made it possible to produce laser pulses with peak intensities exceeding 10^{18} W/cm².[212,213] At such high intensities, the laser can produce a relativistic plasma in which the electric field in the laser focus is so high that electrons are accelerated to near light-speed and interaction with the magnetic component of the electromagnetic wave becomes significant. Under these conditions, electrons perform complicated (quiver) motions in the field and emit electromagnetic radiation at a range of frequencies extending into the hard x-ray region.[213-215] In addition, recombination of electrons with high charge-state ions may occur resulting in the production of narrow bandwidth K_α radiation.[216] Under certain circumstances, these plasmas can also produce very high energy (MeV) electron beams that may be used to study nuclear reactions or to produce hard x-rays through bremsstrahlung.[213] It has also been shown that reverse Thompson scattering of terawatt laser pulses off a high-energy (50 MeV) electron beam can be used to produce hard x-rays (0.4 Å) but with relatively low efficiency.[217]

Ultrafast electron pulses are also useful as a probe for determining the time-dependent structure through diffraction. Electron pulses can be generated using the photoelectric effect followed by electrostatic acceleration into a narrow beam. In recent experiments,[218] this technique has been brought into the sub-picosecond domain. The main problem in maintaining the time-resolution is the space-charge effect: Non-relativistic electrons repel each other through Coulomb repulsion. It is therefore of the greatest importance to accelerate the electrons as quickly as possible and to keep the number of electrons per pulse as low as possible. Thus, it was seen experimentally[219] that for a 100-μm laser spot size on the photocathode, the electron pulse would broaden to about 15 ps when there were as few as 1000 electrons in the pulse. By reducing the number of electrons per pulse and increasing the laser repetition rate, it may be possible to achieve femtosecond resolution in ultrafast electron diffraction experiments.

A series of (sub)picosecond time-resolved electron-diffraction experiments have recently been performed on gas-phase samples in a molecular beam.[218] Two-dimensional electron-diffraction patterns were recorded as a function of pump-probe delay with sub-picosecond time resolution. In these experiments, dissociation reactions in, for example, CF_2I_2, $Fe(CO)_5$, and small cyclic hydrocarbons were studied. The method allowed the observation of rare reaction intermediates and, most importantly, the determination of their spatial structure.

Generating femtosecond hard x-ray pulses is much more difficult than generating electron pulses, which may explain the small number of unique time-resolved diffraction experiments.[214,215] All ultrafast x-ray diffraction experiments to date[58,214,215,220-225] have studied the lattice expansion of semiconductors, metals or organic films under intense laser irradiation. In such an experiment, one typically selects one diffraction peak and measures the intensity of diffracted x rays as a function of the pump-probe delay or the shift or broadening of the diffraction peak. A shift of the diffraction peak is caused by lattice expansion (or, in the presence of shock waves, compression) and a decrease of intensity indicates a loss of crystalline order.[215] Ultrafast x-ray diffraction comes with unique complications. For example, to maintain a high time resolution, the pump beam and x-ray probe beam have to be nearly collinear, restricting the experimental geometry. Also, taking a single diffraction pattern (at one pump-probe delay time or at one orientation of the crystal under study) may take several laser shots. It has been estimated[215] that taking a diffraction pattern of a protein might take as much as seven hours. This makes it very difficult to apply the standard Bragg method in which diffraction patterns are taken for several crystal orientations. Therefore, it will take significant further development of the technology before femtosecond x-ray diffraction will become more commonplace.

D6.3.13   Acknowledgements

D6.3.14 References

(1) Beddard, G. S. *Reports on Progress in Physics* **1993**, *56*, 63.

(2) Paul, P. M.; Toma, E. S.; Breger, P.; Mullot, G.; Auge, F.; Balcou, P.; Muller, H. G.; Agostini, P. *Science* **2001**, *292*, 1689.

(3) Hentschel, M.; Kienberger, R.; Spielmann, C.; Reider, G. A.; Milosevic, N.; Brabec, T.; Corkum, P.; Heinzmann, U.; Drescher, M.; Krausz, F. *Nature* **2001**, *414*, 509.

(4) Krausz, F. *Phys. World* **2001**, *14*, 41.

(5) Service, R. F. *Science* **2001**, *292*, 1627.

(6) Likforman, J.-P.; Mehendale, M.; Villeneuve, D. M.; Joffre, M.; Corkum, P. B. *Opt. Lett.* **2001**, *26*, 99.

(7) Durfee, C. G.; Backus, S.; Kapteyn, H. C.; Murnane, M. M. *Optics Letters* **1999**, *24*, 697.

(8) Kaplan, A. E.; Shkolnikov, P. L. *Phys. Rev. Lett.* **2002**, *88*, 074801.

(9) Saruka, N.; Liu, Z.; Ohtake, H.; Izumida, S.; Yamanaka, T.; Segawa, Y.; Itatani, T.; Sugaya, T.; Nakagawa, T.; Sugiyama, Y. "Saturable Bragg Reflector in a Mode-Locked Laser as an Intracavity THz-Radiation Emitter"; CLEO/QELS'97 Technical Digest, 1997, Baltimore, USA.

(10) Williams, R. M.; Zipfel, W. R.; Webb, W. W. *Curr. Opin. Chem. Biol.* **2001**, *5*, 603.

(11) Nakashima, N.; Shimizu, S.; Yatsuhashi, T.; Sakabe, S.; Izawa, Y. *J. Photochem. Photobiol., C* **2000**, *1*, 131.

(12) Veiko, V. P. *Proc. SPIE-Int. Soc. Opt. Eng.* **2000**, *4088*, 9.

(13) Juhasz, T.; Loesel, F. H.; Kurtz, R. M.; Horvath, C.; Bille, J. F.; Mourou, G. *IEEE J. Sel. Top. Quantum Electron.* **1999**, *5*, 902.

(14) Kurtz, R. M.; Horvath, C.; Liu, H. H.; Krueger, R. R.; Juhasz, T. *J. refrac. surg.* **1998**, *14*, 541.

(15) Lenzner, M.; Krüger, J.; Sartania, S.; Cheng, Z.; Spielmann, C.; Mourou, G.; Kautek, W.; Krausz, F. *Phys. Rev. Lett.* **1998**, *80*, 4076.

(16) Niemz, M. H. *Proc. SPIE-Int. Soc. Opt. Eng.* **1998**, *3255*, 84.

(17) Kohns, P.; Zhou, P.; Stormann, R. *J. Laser Applic.* **1997**, *9*, 171.

(18) Spence, D. E.; Kean, P. N.; Sibbett, W. *Opt. Lett.* **1991**, *16*, 42.

(19) Strickland, D.; Mourou, G. *Opt. Commun.* **1985**, *55*, 447.

(20) Ripin, D. J.; Chudoba, C.; Gopinath, J. T.; Fujimoto, J. G.; Ippen, E. P.; Morgner, U.; Kartner, F. X.; Scheuer, V.; Angelow, G.; Tschudi, T. *Opt. Lett.* **2002**, *27*, 61.

(21) Uemura, S.; Torizuka, K. *OSA Trends Opt. Photonics Ser.* **1999**, *26*, 410.

(22) Chudoba, C.; Fujimoto, J. G.; Ripin, D. J.; Ippen, E. P.; Haus, H. A.; Morgner, U.; Kartner, F. X.; Scheuer, V.; Angelow, G.; Tschudi, T. *Opt. Lett.* **2001**, *26*, 292.

(23) Gayen, S. K.; Zevallos, M. E.; Alrubaiee, M.; Evans, J. M.; Alfano, R. R. *Appl. Opt.* **1998**, *37*, 5327.

(24) Tearney, G. J.; Bouma, B. E.; Boppart, S. A.; Golubovic, B.; Swanson, E. A.; Fujimoto, J. G. *Opt. Lett.* **1996**, *21*, 1408.

(25) Barty, C. P. J.; Gordon, C. L.; Lemoff, B. E. *Opt. Lett.* **1994**, *19*, 1442.

(26) Wynne, K.; Reid, G. D.; Hochstrasser, R. M. *Opt. Lett.* **1994**, *19*, 895.

(27) Backus, S.; Durfee, C. G.; Mourou, G.; Kapteyn, H. C.; Murnane, M. M. *Opt. Lett.* **1997**, *22*, 1256.

(28) Backus, S.; Peatross, J.; Huang, C. P.; Murnane, M. M.; Kapteyn, H. C. *Opt. Lett.* **1995**, *20*, 2000.

(29) Barty, C. P. J.; Korn, G.; Raksi, F.; Rose-Petruck, C.; Squier, J.; Tien, A.-C.; Wilson, K. R.; Yakovlev, V. V.; Yamakawa, K. *Opt. Lett.* **1996**, *21*, 219.

(30) Squier, J.; Barty, C. P. J.; Salin, F.; LeBlanc, C.; Kane, S. *Appl. Opt.* **1998**, *37*, 1638.

(31) Chambaret, J. P.; LeBlanc, C.; Cheriaux, G.; Curley, P.; Darpentigny, G.; Rousseau, P.; Hamoniaux, G.; Antonetti, A.; Salin, F. *Opt. Lett.* **1996**, *21*, 1921.

(32) Rudd, J. V.; Korn, G.; Kane, S.; Squier, J.; Mourou, G.; Bado, P. *Opt. Lett.* **1993**, *18*, 2044.

(33) Reid, G. D.; Wynne, K. Ultrafast Laser Technology and Spectroscopy. In *Encyclopedia of Analytical Chemistry*; Meyers, R. A., Ed.; John Wiley & Sons Ltd: Chichester, 2000; pp 13644.

(34) Backus, S.; Durfee, C. G., III; Murnane, M. M.; Kapteyn, H. C. *Rev. Sci. Instrum.* **1998**, *69*, 1207.

(35) Mourou, G. *Appl. Phys. B* **1997**, *B65*, 205.

(36) Wang, H.; Backus, S.; Chang, Z.; Wagner, R.; Kim, K.; Wang, X.; Umstadter, D.; Lei, T.; Murnane, M.; Kapteyn, H. *J. Opt. Soc. Am. B* **1999**, *16*, 1790.

(37) Backus, S.; Bartels, R.; Thompson, S.; Dollinger, R.; Kapteyn, H. C.; Murnane, M. M. *Opt. Lett.* **2001**, *26*, 465.

(38) Zeek, E.; Bartels, R.; Murnane, M. M.; Kapteyn, H. C.; Backus, S.; Vdovin, G. *Opt. Lett.* **2000**, *25*, 587.

(39) Porter, G. *Proc. Roy. Soc.* **1950**, *A200*, 284.

(40) Kimura, Y.; Alfano, J. C.; Walhout, P. K.; Barbara, P. F. *J. Phys. Chem.* **1994**, *98*, 3450.

(41)   Wynne, K.; Hochstrasser, R. M. *Chem. Phys.* **1995**, *193*, 211.
(42)   Dhar, L.; Rogers, J. A.; Nelson, K. A. *Chemical Reviews* **1994**, *94*, 157.
(43)   Gerstner, V.; Knoll, A.; Pfeiffer, W.; Thon, A.; Gerber, G. *J. Appl. Phys.* **2000**, *88*, 4851.
(44)   Feldstein, M. J.; Vöhringer, P.; Wang, W.; Scherer, N. F. *J. Phys. Chem.* **1996**, *100*, 4739.
(45)   Nunes, G.; Freeman, M. R. *Science* **1993**, *262*, 1029.
(46)   Steeves, G. M.; Elezzabi, A. Y.; Freeman, M. R. *Applied Physics Letters* **1998**, *72*, 504.
(47)   Botkin, D.; Glass, J.; Chemla, D. S.; Ogletree, D. F.; Salmeron, M.; Weiss, S. *Applied Physics Letters* **1996**, *69*, 1321.
(48)   Yang, K. H.; Richards, P. L.; Shen, Y. R. *Appl. Phys. Lett.* **1971**, *19*, 320.
(49)   Benicewicz, P. K.; Taylor, A. J. *Opt. Lett.* **1993**, *18*, 1332.
(50)   Smith, P. R.; Auston, D. H.; Nuss, M. C. *IEEE J. Quantum Electron.* **1988**, *24*, 255.
(51)   Grischkowsky, D.; Keiding, S.; Exter, M., van; Fattinger, C. *J. Opt. Soc. Am.* **1990**, *B7*, 2006.
(52)   You, D.; Jones, R. R.; Bucksbaum, P. H.; Dykaar, D. R. *Opt. Lett.* **1993**, *18*, 290.
(53)   Loeffler, T.; Jacob, F.; Roskos, H. G. *Appl. Phys. Lett.* **2000**, *77*, 453.
(54)   Cook, D. J.; Hochstrasser, R. M. *Opt. Lett.* **2000**, *25*, 1210.
(55)   Hashimshony, D.; Zigler, A.; Papadopoulos, K. *Review of Scientific Instruments* **2000**, *71*, 2380.
(56)   Hashimshony, D.; Zigler, A.; Papadopoulos, K. *Phys. Rev. Lett.* **2001**, *86*, 2806.
(57)   Beard, M. C.; Turner, G. M.; Schmuttenmaer, C. A. *J. Am. Chem. Soc.* **2000**, *112*, 11541.
(58)   RosePetruck, C.; Jimenez, R.; Guo, T.; Cavalleri, A.; Siders, C. W.; Raksi, F.; Squier, J. A.; Walker, B. C.; Wilson, K. R.; Barty, C. P. J. *Nature* **1999**, *398*, 310.
(59)   Weling, A. S.; Hu, B. B.; Froberg, N. M.; Auston, D. H. *Appl. Phys. Lett.* **1994**, *64*, 137.
(60)   Nahata, A.; Auston, D. H.; Wu, C.; Yardley, J. T. *Appl. Phys. Lett.* **1995**, *67*, 1358.
(61)   Han, P. Y.; Tani, M.; Pan, F.; Zhang, X.-C. *Opt. Lett.* **2000**, *25*, 675.
(62)   Hashimoto, H.; Takahashi, H.; Yamada, T.; Kuroyanagi, K.; Kobayashi, T. *J. Phys.* **2001**, *13*, L529.
(63)   Carey, J. J.; Bailey, R. T.; Wynne, K. *Appl. Phys. Lett.* **submitted**.
(64)   Nahata, A.; Weling, A. S.; Heinz, T. F. *Appl. Phys. Lett.* **1996**, *69*, 2321.
(65)   Wu, Q.; Zhang, X.-C. *Appl. Phys. Lett.* **1997**, *70*, 1784.
(66)   Gallot, G.; Grischkowsky, D. *J. Opt. Soc. Am. B* **1999**, *16*, 1204.
(67)   Fluck, R.; Jung, I. D.; Zhang, G.; Kaertner, F. X.; Keller, U. *Opt. Lett.* **1996**, *21*, 743.
(68)   Jiang, Z.; Zhang, X.-C. *Appl. Phys. Lett.* **1998**, *72*, 1945.
(69)   Shan, J.; Weling, A. S.; Knoesel, E.; Bartels, L.; Bonn, M.; Nahata, A.; Reider, G. A.; Heinz, T. F. *Opt. Lett.* **2000**, *25*, 426.
(70)   Park, S.-G.; Melloch, M. R.; Weiner, A. M. *IEEE Journal of Quantum Electronics* **1999**, *35*, 810.
(71)   Leitenstorfer, A.; Hunsche, S.; Shah, J.; Nuss, M. C.; Knox, W. H. *Appl. Phys. Lett.* **1999**, *74*, 1516.
(72)   Kono, S.; Tani, M.; Gu, P.; Sakai, K. *Appl. Phys. Lett.* **2000**, *77*, 4104.
(73)   Nymand, T. M.; Rønne, C.; Keiding, S. *J. Chem. Phys.* **2001**, *114*, 5246.
(74)   Venables, D. S.; Schmuttenmaer, C. A. *J. Chem. Phys.* **2000**, *113*, 11222.
(75)   Huggard, P. G.; Cluff, J. A.; Shaw, C. J.; Andrews, S. R.; Linfield, E. H.; Ritchie, D. A. *Appl. Phys. Lett.* **1997**, *71*, 2647.
(76)   Leitenstorfer, A.; Hunsche, S.; Shah, J.; Nuss, M. C.; Knox, W. H. *Phys. Rev. B* **2000**, *61*, 16642.
(77)   Kersting, R.; Bratschitsch, R.; Strasser, G.; Unterainer, K.; Heyman, J. N. *Opt. Lett.* **2000**, *25*, 272.
(78)   Wynne, K.; Jaroszynski, D. A. *Opt. Lett.* **1999**, *24*, 25.
(79)   Wynne, K.; Carey, J. J.; Zawadzka, J.; Jaroszynski, D. A. *Opt. Commun.* **2000**, *176*, 429.
(80)   Carey, J. J.; Zawadzka, J.; Jaroszynski, D. A.; Wynne, K. *Phys. Rev. Lett.* **2000**, *84*, 1431.
(81)   Mitrofanov, O.; Lee, M.; Hsu, J. W. P.; Pfeiffer, L. N.; West, K. W.; Wynn, J. D. *Appl. Phys. Lett.* **2001**, *79*, 907.
(82)   Zhang, W.; Zhang, J.; Grischkowsky, D. *Appl. Phys. Lett.* **2001**, *78*, 2425.
(83)   Han, P. Y.; Cho, G. C.; Zhang, X.-C. *Opt. Lett.* **2000**, *25*, 242.
(84)   McGowan, R. W.; Cheville, R. A.; Grischkowsky, D. *Appl. Phys. Lett.* **2000**, *76*, 670.
(85)   Ruffin, A. B.; Decker, J.; Sanchez-Palencia, L.; Hors, L. L.; Whitaker, J. F.; Norris, T. B.; Rudd, J. V. *Opt. Lett.* **2001**, *26*, 681.
(86)   Raman, C.; Conover, C. W. S.; Sukenik, C. I.; Bucksbaum, P. H. *Phys. Rev. Lett.* **1996**, *76*, 2436.
(87)   Wesdorp, C.; Robicheaux, F.; Noordam, L. D. *Phys. Rev. Lett.* **2001**, *87*, 83001.
(88)   Saeta, P. N.; Federici, J. F.; Greene, B. I.; Dykaar, D. R. *Appl. Phys. Lett.* **1992**, *60*, 1477.
(89)   Zielbauer, J.; Wegener, M. *Appl. Phys. Lett.* **1996**, *68*, 1223.
(90)   Beard, M. C.; Turner, G. M.; Schmuttenmaer, C. A. *Phys. Rev. B* **2000**, *62*, 15764.
(91)   Schall, M.; Jepsen, P. U. *Opt. Lett.* **2000**, *25*, 13.
(92)   Haran, G.; Sun, W. D.; Wynne, K.; Hochstrasser, R. M. *Chemical Physics Letters* **1997**, *274*, 365.
(93)   McElroy, R.; Wynne, K. *Phys. Rev. Lett.* **1997**, *79*, 3078.
(94)   Flanders, B. N.; Arnett, D. C.; Scherer, N. F. *IEEE J. Selec. Top. Quantum. Opt.* **1998**, *4*, 353.
(95)   McElroy, R.; Wynne, K. *Laser Chem.* **1999**, *19*, 145.

(96)   Kindt, J. T.; Schmuttenmaer, C. A. *Journal of Chemical Physics* **1999**, *110*, 8589.

(97)   Ware, B.; Williamson, K.; Devlin, J. P. *J. Phys. Chem.* **1968**, *72*, 3970.

(98)   Birch, D. J. S.; Imhof, R. E. Time-Domain Fluorescence Spectroscopy Using Time-Correlated Single Photon Counting. In *Topics in Fluorescence Spectroscopy*; Lakowicz, J. R., Ed.; Plenum Press: New York, 1991; Vol. 1 Techniques; pp 1.

(99)   O'Connor, D. V.; Phillips, D. *Time-Correlated Single Photon Counting*; Academic Press: New York, 1984.

(100)   Rosker, M. J.; Rose, T. S.; Zewail, A. H. *Chem. Phys. Lett.* **1988**, *146*, 175–179.

(101)   Gadella, T. W. J. J.; Jovin, T. M.; Clegg, R. M. *Biophys. Chem.* **1993**, *48*, 221.

(102)   Szmacinski, H.; Lakowicz, J. R.; Johnson, M. L. *Methods Enzymol.* **1994**, *240*, 723.

(103)   Wang, X. F.; Uchida, T.; Coleman, D. M.; Minami, S. *Appl. Spectrosc.* **1991**, *45*, 360.

(104)   Sytsma, J.; Vroom, J. M.; De Grauw, C. J.; Gerritsen, H. C. *J. Microsc.* **1998**, *191*, 39.

(105)   Szmacinski, H.; Lakowicz, J. R. *Sensors and Actuators B* **1995**, *29*, 16.

(106)   Benny Lee, K. C.; Siegel, J.; Webb, S. E. D.; Leveque-Fort, S.; Cole, M. J.; Jones, R.; Dowling, K.; Lever, M. J.; French, P. M. W. *Biophys. J.* **2001**, *81*, 1265.

(107)   Verveer, P. J.; Squire, A.; Bastiaens, P. I. H. *Biophys. J.* **2000**, *78*, 2127.

(108)   Bastiaens, P. I. H.; Squire, A. *Trends in Cell Biology* **1999**, *9*, 48.

(109)   Nishimura, C.; Riley, R.; Eastman, P.; Fink, A. L. *J. Mol. Biol.* **2000**, *299*, 1133.

(110)   Lakshmikanth, G. S.; Sridevi, K.; Krishnamoorthy, G.; Udgaonkar, J. B. *Nat. Struct. Biol.* **2001**, *8*, 799.

(111)   Ng, T.; Squier, A.; Hansra, G.; Bornancin, F.; Prevostel, C.; Hanby, A.; Harris, W.; Barnes, D.; Schmidt, D.; Mellor, H.; Bastiaens, P. I. H.; Parker, P. J. *Science* **1999**, *283*, 2085.

(112)   Xie, X. S.; Trautman, J. K. *An. Rev. Phys. Chem.* **1998**, *49*, 441.

(113)   Moerner, W. E. *J. Phys. Chem. B* **2002**, *106*, 910.

(114)   Moerner, W. E.; Orrit, M. *Science* **1999**, *283*, 1670.

(115)   Weston, K. D.; Goldner, L. S. *J. Phys. Chem. B* **2001**, *105*, 3453.

(116)   Eggeling, C.; Fries, J. R.; Brand, L.; Gunther, R.; Seidel, C. A. M. *Proc. Natl. Acad. Sci.* **1998**, *95*, 1556.

(117)   Fries, J. R.; Brand, L.; Eggeling, C.; Koellner, M.; Seidel, C. A. M. *J. Phys. Chem. A* **1998**, *102*, 6601.

(118)   Schaffer, J.; Volkmer, A.; Eggeling, C.; Subramaniam, V.; Striker, G.; Seidel, C. A. M. *J. Phys. Chem. A* **1999**, *103*, 331.

(119)   Betzig, E.; Trautman, J. K. *Science* **1992**, *257*, 189.

(120)   Basche, T.; Kummer, S.; Brauchle, C. *Nature* **1995**, *373*, 132.

(121)   Simoni, E.; Reber, C.; Talaga, D.; Zink, J. I. *J. Phys. Chem.* **1993**, *97*, 12678.

(122)   Mahr, H.; Hirsch, M. D. *Opt. Commun.* **1975**, *13*, 96.

(123)   Kahlow, M. A.; Jarzeba, W.; DuBruil, T. P.; Barbara, P. F. *Rev. Sci. Instrum.* **1988**, *59*, 1098.

(124)   Kennis, J. T. M.; Gobets, B.; van Stokkum, I. H. M.; Dekker, J. P.; van Grondelle, R.; Fleming, G. R. *J. Phys. Chem. B* **2001**, *105*, 4485.

(125)   Rubtsov, I. V.; Yoshihara, K. *J. Phys. Chem. A* **1999**, *103*, 10202.

(126)   Fiebig, T.; Chachisvilis, M.; Manger, M.; Zewail, A. H.; Douhal, A.; Garcia-Ochoa, I.; de La Hoz Ayuso, A. *J. Phys. Chem. A* **1999**, *103*, 7419.

(127)   Kovalenko, S. A.; Schanz, R.; Fartzdinov, V. M.; Hennig, H.; Ernsting, N. P. *Chem. Phys. Lett.* **2000**, *323*, 312.

(128)   Rubtsov, I. V.; Yoshihara, K. *J. Phys. Chem. A* **1997**, *101*, 6138.

(129)   Zewail, A. H. *Ang. Chem. Int. Ed.* **2001**, *40*, 4371.

(130)   Zewail, A. H. *The Chemical Bond. Structure and Dynamics*; Academic Press: Boston, 1992.

(131)   Zewail, A. H. *Femtochemistry: Ultrafast dynamics of the chemical bond*; World Scientific: Singapore, 1994; Vol. 3.

(132)   Stolow, A. *Philos. Trans. R. Soc. London, Ser. A* **1998**, *356*, 345.

(133)   Vrakking, M. J. J.; Villeneuve, D. M.; Stolow, A. *J. Chem. Phys.* **1996**, *105*, 5647.

(134)   Vrakking, M. J. J.; Villeneuve, D. M.; Stolow, A. *Phys. Rev. A* **1996**, *54*, R37.

(135)   Averbukh, I. S.; Vrakking, M. J. J.; Villeneuve, D. M.; Stolow, A. *Phys. Rev. Lett.* **1996**, *77*, 3518.

(136)   Rice, S. A.; Tannor, D. J.; Kosloff, R. *J. Chem. Soc., Faraday Trans. 2* **1986**, *82*, 2423.

(137)   Tannor, D. J.; Rice, S. A. *Adv. Chem. Phys.* **1988**, *70*, 441.

(138)   Stockman, M. I.; Faleev, S. V.; Bergman, D. J. *Phys. Rev. Lett.* **2002**, *88*, 067402/1.

(139)   Brixner, T.; Damrauer, N. H.; Niklaus, P.; Gerber, G. *Nature* **2001**, *414*, 57.

(140)   Dantus, M. *Annu. Rev. Phys. Chem.* **2001**, *52*, 639.

(141)   Engel, V.; Schinke, R.; Hennig, S.; Metiu, H. *J. Chem. Phys.* **1990**, *92*, 1.

(142)   Uberna, R.; Amitay, Z.; Loomis, R. A.; Leone, S. R. *Faraday Discuss.* **1999**, *113*, 385.

(143)   Tannor, D. J.; Kosloff, R.; Rice, S. A. *J. Chem. Phys.* **1986**, *85*, 5805.

(144)   Brumer, P.; Shapiro, M. *J. Chem. Phys.* **1986**, *84*, 4103.

(145)   Bardeen, C. J.; Yakovlev, V. V.; Wilson, K. R.; Carpenter, S. D.; Weber, P. M.; Warren, W. S. *Chem. Phys. Lett.* **1997**, *280*, 151.

(146)   Judson, R. S.; Rabitz, H. *Phys. Rev. Lett.* **1992**, *68*, 1500.

(147)   Levis, R. J.; Menkir, G. M.; Rabitz, H. *Science* **2001**, *292*, 709.

(148)   Assion, A.; Baumert, T.; Bergt, M.; Brixner, T.; Kiefer, B.; Seyfried, V.; Strehle, M.; Gerber, G. *Science* **1998**, *282*, 919.

(149)   Weinacht, T. C.; White, J. L.; Bucksbaum, P. H. *J. Phys. Chem. A* **1999**, *103*, 10166.

(150)   Voth, G. A.; Hochstrasser, R. M. *Journal of Physical Chemistry* **1996**, *100*, 13034.

(151)   Pugliano, N.; Szarka, A. Z.; Hochstrasser, R. M. *J. Chem. Phys.* **1996**, *104*, 5062.

(152)   Bursing, H.; Vohringer, P. *Phys. Chem. Chem. Phys.* **2000**, *2*, 73.

(153)   Hess, S.; Bursing, H.; Vohringer, P. *J. Chem. Phys.* **1999**, *111*, 5461.

(154)   Wang, Z.; Wasserman, T.; Gershgoren, E.; Vala, J.; Kosloff, R.; Ruhman, S. *Chem. Phys. Lett.* **1999**, *313*, 155.

(155)   Gershgoren, E.; Banin, U.; Ruhman, S. *J. Phys. Chem. A* **1998**, *102*, 9.

(156)   Ashkenazi, G.; Banin, U.; Bartana, A.; Kosloff, R.; Ruhman, S. *Adv. Chem. Phys.* **1997**, *100*, 229.

(157)   Scherer, N. F.; Ziegler, L. D.; Fleming, G. R. *J. Chem. Phys.* **1992**, *96*, 5544–5547.

(158)   Yan, Y.; Whitnell, R. M.; Wilson, K. R.; Zewail, A. H. *Chem. Phys. Lett.* **1992**, *193*, 402.

(159)   Bargheer, M.; Guehr, M.; Dietrich, P.; Schwentner, N. *Physical Chemistry Chemical Physics* **2002**, *4*, 75.

(160)   Davis, A. V.; Wester, R.; Bragg, A. E.; Neumark, D. M. *Abstr. Pap. - Am. Chem. Soc.* **2001**, *221st*, PHYS.

(161)   Wynne, K.; Hochstrasser, R. M. *Adv. Chem. Phys.* **1999**, *107*, 263.

(162)   Wynne, K.; Reid, G. D.; Hochstrasser, R. M. *J. Chem. Phys.* **1996**, *105*, 2287.

(163)   Petrich, J. W.; Martin, J. L.; Houde, D.; Poyart, C.; Orszag, A. *Biochemistry* **1987**, *26*, 7914.

(164)   *Ultrafast infrared and Raman spectroscopy*; Fayer, M. D., Ed.; Marcel Dekker: New York, 2001.

(165)   Laubereau, A.; Fischer, S. F.; Spanner, K.; Kaiser, W. *Chem. Phys.* **1978**, *31*, 335.

(166)   Hochstrasser, R. M. *Proc. SPIE-Int. Soc. Opt. Eng.* **1993**, *1921*, 16.

(167)   Cho, M. *Phys. Chem. Comm.* **2002**, *7*, 1.

(168)   Lian, T.; Bromberg, S. E.; Asplund, M.; Yang, H.; Harris, C. B. *J. Phys. Chem.* **1996**, *100*, 11994.

(169)   Asplund, M. C.; Yang, H.; Kotz, K. T.; Bromberg, S. E.; Wilkens, M. J.; Harris, C. B. *Laser Chemistry* **1999**, *19*, 253.

(170)   Payne, C. K.; Snee, P. T.; Yang, H.; Kotz, K. T.; Schafer, L. L.; Tilley, T. D.; Harris, C. B. *J. Am. Chem. Soc.* **2001**, *123*, 7425.

(171)   Kotz, K. T.; Yang, H.; Snee, P. T.; Payne, C. K.; Harris, C. B. *J. Organomet. Chem.* **2000**, *596*, 183.

(172)   Woutersen, S.; Emmerichs, U.; Bakker, H. J. *Laser Chem.* **1999**, *19*, 83.

(173)   Yang, H.; Snee, P. T.; Kotz, K. T.; Payne, C. K.; Harris, C. B. *J. Am. Chem. Soc.* **2001**, *123*, 4204.

(174)   Omta, A. W.; Kropman, M. F.; Woutersen, S.; Bakker, H. J. *Science* **2003**, *301*, 347.

(175)   Hamm, P.; Zinth, W. *J. Phys. Chem.* **1995**, *99*, 13537.

(176)   Dziewior, R.; Diller, R. *Ber. Bunsen-Ges.* **1996**, *100*, 2103.

(177)   Hamm, P.; Lim, M.; Hochstrasser, R. M. *J. Phys. Chem. B* **1998**, *102*, 6123.

(178)   Asbury, J. B.; Hao, E.; Wang, Y.; Lian, T. *J. Phys. Chem. B* **2000**, *104*, 11957.

(179)   Elsaesser, T.; Nuss, M. C. *Opt. Lett.* **1991**, *16*, 411.

(180)   Murphy, R. E.; Cook, F. H.; Sakai, H. *J. Opt. Soc. Am.* **1975**, *65*, 600.

(181)   Sakai, H.; Murphy, R. E. *Appl. Opt.* **1978**, *17*, 1342.

(182)   Carey, J. J.; Bailey, R. T.; Pugh, D.; Sherwood, J. N.; Cruickshank, F. R.; Wynne, K. *Appl. Phys. Lett.* **2002**, *81*, 4335.

(183)   Smith, G. D.; Hutson, M. S.; Lu, Y.; Tierney, M. T.; Grinstaff, M. W.; Palmer, R. A. *Appl. Spectrosc.* **2001**, *55*, 637.

(184)   Brudler, R.; Rammelsberg, R.; Woo, T. T.; Getzoff, E. D.; Gerwert, K. *Nat. Struct. Biol.* **2001**, *8*, 265.

(185)   Hu, X.; Frei, H.; Spiro, T. G. *Biochemistry* **1996**, *35*, 13001.

(186)   Cola, L. d.; Barigelletti, F.; Balzani, V.; Hage, R.; Haasnoot, J. G.; Reedijk, J.; Vos, J. G. *Chem. Phys. Lett.* **1991**, *178*, 491.

(187)   Sun, X. Z.; Nikiforov, S. M.; Yang, J.; Colley, C. S.; George, M. W. *Appl. Spectrosc.* **2002**, *56*, 31.

(188)   Kramers, H. A. *Physica* **1940**, *7*, 287.

(189)   Marcus, R. A.; Sutin, N. *Biochim. et Biophys. Acta* **1985**, *811*, 265.

(190)   Sumi, H.; Marcus, R. A. *J. Chem. Phys.* **1986**, *84*, 4894.

(191)   Fragnito, H. L.; Bigot, J.-Y.; Becker, P. C.; Shank, C. V. *Chem.Phys.Lett.* **1989**, *160*, 101.

(192)   Nibbering, E. T. J.; Wiersma, D. A.; Duppen, K. *Phys.Rev.Lett.* **1991**, *66*, 2464.

(193)   Beddard, G. S.; McFadyen, G. G.; Reid, G. D.; Thorne, J. R. G. *Chem. Phys.* **1993**, *172*, 363.

(194)   Voehringer, P.; Arnett, D. C.; Westervelt, R. A.; Feldstein, M. J.; Scherer, N. F. *J. Chem. Phys.* **1995**, *102*, 4027.

(195)   Fleming, G. R.; Joo, T.; Cho, M. *Adv. Chem. Phys.* **1997**, *101*, 141.

(196)   de Boeij, W. P.; Pshenichnikov, M. S.; Wiersma, D. A. *Chemical Physics* **1998**, *233*, 287.

(197)   Asplund, M. C.; Zanni, M. T.; Hochstrasser, R. M. *Proc. Natl. Acad. Sci. U. S. A.* **2000**, *97*, 8219.

(198)   Golonzka, O.; Demirdoven, N.; Khalil, M.; Tokmakoff, A. *Journal of Chemical Physics* **2000**, *113*, 9893.

(199)   Merchant, K. A.; Thompson, D. E.; Fayer, M. D. *Phys. Rev. Lett.* **2001**, *86*, 3899.

(200)   Ge, N.-H.; Hochstrasser, R. M. *Phys. Chem. Comm.* **2002**, *3*, 1.
(201)   Dantus, M.; Janssen, M. H. M.; Zewail, A. H. *Chem. Phys. Lett.* **1991**, *181*, 281.
(202)   Assion, A.; Baumert, T.; Geisler, M.; Seyfried, V.; Gerber, G. *Eur. Phys. J. D* **1998**, *4*, 145.
(203)   Pedersen, J. E.; Keiding, S. R. *IEEE J. Quantum Electron.* **1992**, *28*, 2518.
(204)   Horn, B. A.; Herek, J. L.; Zewail, A. H. *J. Am. Chem. Soc.* **1996**, *118*, 8755.
(205)   Kim, S. K.; Pedersen, S.; Zewail, A. H. *J. Chem. Phys.* **1995**, *103*, 477.
(206)   Diau, E. W. G.; DeFeyter, S.; Zewail, A. H. *Chemical Physics Letters* **1999**, *304*, 134.
(207)   Zhong, D.; Ahmad, S.; Zewail, A. H. *J. Am. Chem. Soc.* **1997**, *119*, 5978.
(208)   De Feyter, S.; Diau, E. W. G.; Zewail, A. H. *Phys. Chem. Chem. Phys.* **2000**, *2*, 877.
(209)   Koetting, C.; Diau, E. W. G.; Baldwin, J. E.; Zewail, A. H. *J. Phys. Chem. A* **2001**, *105*, 1677.
(210)   Rundquist, A.; Durfee, C. G.; Chang, Z. H.; Herne, C.; Backus, S.; Murnane, M. M.; Kapteyn, H. C. *Science* **1998**, *280*, 1412.
(211)   Lenzner, M.; Schnuerer, M.; Spielmann, C.; Krausz, F. *IEICE Trans. Electron.* **1998**, *E81-C*, 112.
(212)   Yamakawa, K.; Barty, C. P. J. *IEEE J. Sel. Top. Quantum Electron.* **2000**, *6*, 658.
(213)   Umstadter, D. *Phys. Plasmas* **2001**, *8*, 1774.
(214)   Wark, J. *Contemp. Phys.* **1996**, *37*, 205.
(215)   Rousse, A.; Rischel, C.; Gauthier, J.-C. *Rev. Mod. Phys.* **2001**, *73*, 17.
(216)   Guo, T.; Spielmann, C.; Walker, B. C.; Barty, C. P. J. *Rev. Sci. Instrum.* **2001**, *72*, 41.
(217)   Schoenlein, R. W.; Leemans, W. P.; Chin, A. H.; Volfbeyn, P.; Glover, T. E.; Balling, P.; Zolotorev, M.; Kim, K. J.; Chattopadhyay, S.; Shank, C. V. *Science* **1996**, *274*, 236.
(218)   Ruan, C. Y.; Lobastov, V. A.; Srinivasan, R.; Goodson, B. M.; Ihee, H.; Zewail, A. H. *Proc. Natl. Acad. Sci.* **2001**, *98*, 7117.
(219)   Dantus, M.; Kim, S. B.; Williamson, J. C.; Zewail, A. H. *J. Phys. Chem.* **1994**, *98*, 2782.
(220)   Siders, C. W.; Cavalleri, A.; SokolowskiTinten, K.; Toth, C.; Guo, T.; Kammler, M.; vonHoegen, M. H.; Wilson, K. R.; vonderLinde, D.; Barty, C. P. J. *Science* **1999**, *286*, 1340.
(221)   Chin, A. H.; Schoenlein, R. W.; Glover, T. E.; Balling, P.; Leemans, W. P.; Shank, C. V. *Phys. rev. Lett.* **1999**, *83*, 336.
(222)   Lindenberg, A. M.; Kang, I.; Johnson, S. L.; Missalla, T.; Heimann, P. A.; Chang, Z.; Larsson, J.; Bucksbaum, P. H.; Kapteyn, H. C.; Padmore, H. A.; Lee, R. W.; Wark, J. S.; Falcone, R. W. *Physical Review Letters* **2000**, *84*, 111.
(223)   Cavalleri, A.; Siders, C. W.; Brown, F. L. H.; Leitner, D. M.; Tóth, C.; Squier, J. A.; Barty, C. P. J.; Wilson, K. R.; Sokolowski-Tinten, K.; Hoegen, M. H. v.; Linden, D. v. d.; Kammler, M. *Phys. Rev. Lett.* **2000**, *85*, 586.
(224)   Reis, D. A.; DeCamp, M. F.; Bucksbaum, P. H.; Clarke, R.; Dufresne, E.; Hertlein, M.; Merlin, R.; Falcone, R.; Kapteyn, H.; Murnane, M. M.; Larson, J.; Missalla, T.; Wark, J. S. *Phys. Rev. Lett.* **2001**, *86*, 3072.
(225)   Rousse, A.; Rischel, C.; Fourmaux, S.; Uschmann, I.; Sebban, S.; Grillon, G.; Balcou, P.; Foster, E.; Geindre, J. P.; Audebert, P.; Gauthier, J. C.; Hulin, D. *Nature* **2001**, *410*, 65.